Probabilistic Reinforcement Learning in Schizophrenia: Relationships to Anhedonia and Avolition

Supplemental Information

Supplemental Methods and Materials

Exclusion Criteria

Exclusion criteria were 1) DSM-IV substance abuse within the past year, or substance dependence within the past 2 years (except nicotine); 2) DSM-IV major depressive disorder or dysthymia in the past year; 3) any unstable or severe medical disorder; 4) past head injury with neurological sequelae and/or loss of consciousness; 5) DSM-IV mental retardation, and 6) any contraindication to MRI including pregnancy, claustrophobia, any metallic object in the body, history of heart rhythm abnormalities, and presence of a heart pacemaker.

Diagnosis and Clinical Assessment

Participant diagnoses were based on a Structured Clinical Interview for DSM-IV-TR (1) conducted by a Masters-level clinician. Clinical symptoms were rated using the Scales for the Assessment of Positive Symptoms (SAPS) (2) and Negative Symptoms (SANS) (3), which were summarized into positive, negative, and disorganization symptoms. Clinician-rated symptoms of anhedonia and avolition were assessed with the SANS and the Brief Negative Symptom Scale (BNSS) (4). Given that anhedonia and avolition scores derived from the SANS correlate significantly with those derived from the BNSS, and that anhedonia and avolition scores load onto a single factor in both scales (4), we created a single score for clinician-rated symptoms of anhedonia and avolition by Z-scoring and summing across measures. Anhedonia and avolition were also assessed using the Revised Chapman Physical and Social Anhedonia Scales (5, 6), the Temporal Experience of Pleasure Scale (7), the Snaith-Hamilton Pleasure Scale (8), and the

Apathy Scale (9), which were Z-scored and summed to create a composite measure of self-reported anhedonia/avolition. Both of these measures – clinician rated and self-reported anhedonia/amotivation – were used in individual difference analyses. Participants were required to pass a urine drug screen and breathalyzer test at the start of each session.

Task

The experimental paradigm was a modified version of the Probabilistic Stimulus Selection Task (Figure 1) (10). The task consisted of an acquisition phase, during which fMRI scanning took place, and a test phase that was completed outside the scanner. Stimuli consisted of grayscale drawings from the revised Snodgrass and Vanderwart object pictorial set (11), matched for luminance and contrast, visual complexity, and object familiarity. Object-condition mappings were counterbalanced across subjects. During the acquisition phase, participants were presented on each trial with one of three pairs of stimuli (“AB”, “CD”, or “EF”), in pseudorandomized order, and were instructed to choose the stimulus in each pair that they believe is ”correct” based on feedback received over time. Stimuli were displayed for 2000 ms, during which the participant was required to choose one of the stimuli via button press. After a jittered interstimulus interval ranging from 2000-6000 ms, feedback consisting of the words “Correct! +$” in green text, “Incorrect $0” in red text, or “Too Slow!” in red text were presented on screen for 2000 ms. Subjects were told that for each “Correct” choice, they would win extra money, with a total of up to $20 available to be won (in actuality, all subjects were paid an additional $20 upon completion). For stimulus pair AB, choice of A was rewarded 80% of the time, while B was rewarded 20% of the time; pair CD was 70:30, and pair EF was 60:40. Feedback was followed by an intertrial interval jittered from 2000-6000 ms. The stimuli were presented in 10 blocks of 36 trials (12 per stimulus pair). Each block (run) took ~7.2 minutes, for a total of ~72 minutes.

The test phase was administered outside of the scanner. In this phase, the three original

stimulus pairs were presented, along with 12 novel pairs in which the 3 original pairs were recombined as in (10). Each pair was presented 10 times, and participants were asked to choose the more frequently rewarded member of each pair based on the knowledge acquired earlier. No feedback was given at this stage. Trials were separated with 1000 ms crosshairs triggered upon response, and no time limit was imposed on test-phase responses (i.e., it was self-paced). As in previous studies using this task (10), the recombined pairs from the test phase were used to calculate transfer measures indicative of learning from positive versus negative outcomes. Because A was the most highly reinforced stimulus during training, a "ChooseA" measure was created by averaging performance on all novel pairs including A was used to indicate Go learning, and an analogous "AvoidB" measure was created to index NoGo learning (see Figure 1).

Given pilot data indicating that individuals with schizophrenia had more difficulty understanding the task than controls, patients underwent a training session within the week prior to scanning where they completed 360 task trials with a different set of stimuli. Both groups also completed a 12-trial practice session immediately before scanning.

Image Acquisition and Processing

Imaging was performed on a 3T Siemens TIM TRIO system with a 12-channel head coil. High-resolution structural images were acquired using a sagittal magnetization-prepared rapid acquisition gradient echo (MP-RAGE) sequence (TR = 2.4 s, TE = 3.08 ms, inversion time = 1 s, flip = 8°, 176 slices, 1 mm^3 voxels). Functional images were collected in 10 runs of 213 frames each using a gradient echo echo-planar sequence (TR = 2030 ms, TE = 27 ms, flip = 90°, 36 slices). Functional runs acquired axial images parallel to the anterior-posterior commissure plane with 4 mm^3 isotopic voxels. Stimuli were presented using E-prime 2.0. The MR data was normalized across runs by scaling whole-brain signal intensity to a fixed value and removing the linear slope on a voxel-by-voxel basis to counteract effects of drift (12). The data

was then aligned to correct for head motion using rigid-body rotation and translation correction algorithms (13-15), which provide estimated absolute and frame-by-frame movement parameters used to evaluate movement differences between groups. Ten individuals with schizophrenia and 4 controls were excluded for excessive movement (see Table S1). After movement correction, the images were resampled into 3 mm^3 voxels, registered to Talairach space using 12-parameter affine transformations, and smoothed with a 6 mm FWHM Gaussian filter.

Model-based fMRI Analyses

Behavioral data was modeled using a Q-learning algorithm with separate learning rates from positive feedback ("gains"; $\propto_G$) and negative feedback ("losses", $\propto_L$) (16). This algorithm models subjects' choices by calculating a Q value, which is an estimate of expected reward value, for each stimulus (A-F). This value is modified on each trial according to the reward $r(t)$ received, where $r(t) = 1$ for positive feedback and $r(t) = 0$ for negative feedback. Expected value for stimulus i on trial $t + 1$ is updated as follows:

$$Q_i(t+1) = Q_i(t) + \propto_G [r(t) - Q_i(t)]_+ + \propto_L [r(t) - Q_i(t)]_-$$

where $[r(t) - Q_i(t)]$, the reward received minus the reward expected, represents prediction error. In other words, the expected value for a given stimulus on a given trial is equal to its expected value on the previous trial plus an adjustment factor equal to prediction error times learning rate. Positive prediction errors (rewards that are higher than expected) are multiplied by the gain learning rate, and negative prediction errors (rewards that are lower than expected) are multiplied by the loss learning rate. Learning rates reflect the degree to which Q values are affected by reinforcement outcomes, with higher learning rates associated with larger changes in Q value on each trial. Action selection was modeled using a softmax logistic function, a standard stochastic decision rule that calculates the probability of choosing one stimulus over

another given the expected reward values of both options:

$$P_A(t) = \frac{e^{\frac{Q_A(t)}{\beta}}}{e^{\frac{Q_A(t)}{\beta}} + e^{\frac{Q_B(t)}{\beta}}}$$

where β is an inverse gain parameter and reflects the participant's tendency to exploit (stick with responses that have yielded reward in the past) vs explore (try out different choices to determine whether a more rewarding option is available). The three free model parameters ($\propto_G$, $\propto_L$,and β) were obtained by fitting the model to each subject's trial-by-trial choices during the training phase to maximize their log likelihood estimate (LLE):

$$LLE = \log(\prod_t P_{i*,t})$$

This was accomplished by the use of standard optimization algorithms from MATLAB's optimization toolbox, with multiple starting points. Model fits for each subject were characterized using LLE values as well as Bayesian Information Criterion (BIC) (17), which penalizes for the number of free parameters used to protect against overfitting. In particular, we checked that the model with gain and loss learning rates fit better than a model with a single learning rate. To validate the quality of the model fit, we used the model with fit parameters to simulate the task. Specifically, for each subject, we ran the model on the task 1000 times with the fit parameters, and then averaged behavior across them. We compared the model simulations with subjects' data quantitatively by plotting model-predicted learning curves (as well as win-stay lose-shift behavior across time) for each pair. We also binned all trials into deciles based on the model-predicted probability of choosing the optimal option, and compared this to the empirically observed probability on those trials.

ANOVA-Based fMRI Analyses

In addition to the computational model based analyses, standard ANOVA-based analyses with trials coded by choice and feedback type were conducted. For these analyses, at the time of

stimulus presentation, 6 choice types were modeled (A, B, C, D, E, and F), and at the time of feedback, 12 feedback types were modeled (positive and negative feedback for each choice). Non-response trials were coded as a variable of no interest. Activation at the time of choice was evaluated using a repeated measures ANOVA with choice type (A/C/E or B/D/F) and time (1-9) as within-subjects factors and group as a between subjects factor. Feedback-related activity was examined using a repeated measures ANOVA with choice type, feedback type (positive, negative), and time as within-subjects factors and group as a between-subjects factor. Choice type was included as a factor in analyses of feedback as an alternative method of evaluating prediction error effects, which would be expected to modulate responses to feedback according to whether the outcome was expected or unexpected. Because several subjects had too little variability in their choices to code all event types, we also created GLMs in which all three stimulus pairs were combined. These GLMs included only two choice types (high-probability (A/C/E), low-probability (B/D/F)), and four feedback types (ACE/positive, ACE/negative, BDF/positive, BDF/negative).

Movement Analysis

Movement parameters including absolute, incremental (frame-to-frame), and mean voxelwise standard deviation values were compared between groups (Table S1), and participants with movement or SD values not meeting predetermined criteria were removed. Specifically, 10 individuals with schizophrenia and 4 healthy controls were excluded for movement that exceeded a mean voxelwise standard deviation value of 20.0 for 4 or more BOLD runs. In addition, one subject chose to end the experiment early and did not complete the final BOLD run or test phase. The resulting sample was well matched for movement between groups. Repeated-measures ANOVAs with BOLD run (1-10) as a within-subjects factor and Group (CON, SCZ) as a between-subjects factor revealed no significant main effects of group or BOLD run X group interactions for any measure of movement (absolute movement, frame-to-frame, or

voxel-wise standard deviation (all *p*s > .27), indicating that movement did not differ between patients and controls.

Table S1. Comparison of movement parameters between groups

Group	BOLD	Incremental		Absolute		Standard Deviation	
		M	SD	M	SD	M	SD
CON	1	0.13	0.07	0.37	0.27	11.34	2.83
	2	0.18	0.19	0.38	0.29	11.83	3.60
	3	0.15	0.09	0.37	0.26	11.76	2.74
	4	0.17	0.14	0.43	0.31	12.50	3.38
	5	0.19	0.12	0.57	0.56	13.69	4.27
	6	0.19	0.12	0.57	0.56	14.15	5.21
	7	0.26	0.29	0.62	0.59	14.15	5.21
	8	0.23	0.20	0.54	0.45	13.77	4.48
	9	0.22	0.23	0.58	0.41	14.28	4.45
	10	0.24	0.21	0.58	0.43	14.14	4.38
SCZ	1	0.17	0.16	0.40	0.46	11.97	4.16
	2	0.18	0.12	0.38	0.35	12.03	3.80
	3	0.20	0.22	0.40	0.36	12.49	4.83
	4	0.18	0.11	0.47	0.38	13.08	3.99
	5	0.19	0.12	0.38	0.31	12.09	3.16
	6	0.21	0.16	0.50	0.54	13.64	4.07
	7	0.21	0.20	0.52	0.63	13.47	4.37
	8	0.24	0.28	0.49	0.60	13.44	5.61
	9	0.24	0.30	0.47	0.45	13.57	4.97
	10	0.20	0.12	0.40	0.21	12.91	3.25

fMRI ANOVA-based Analyses

Feedback analysis

This analysis examined a Choice (A/C/E, B/D/F) x Time (1-9) x Feedback (Positive, Negative) x Group (CON, SCZ) ANOVA. Trials were collapsed across stimulus pair. In the striatal ROI analysis, all regions demonstrated significant Feedback x Time interactions that survived correction for multiple comparisons (all p values < .02). Example timecourses are shown in Figure S1, and demonstrate that both groups activated bilateral caudate, putamen, and nucleus accumbens more strongly for positive than negative feedback. There was no evidence of a reduction in this effect among patients as compared to controls.

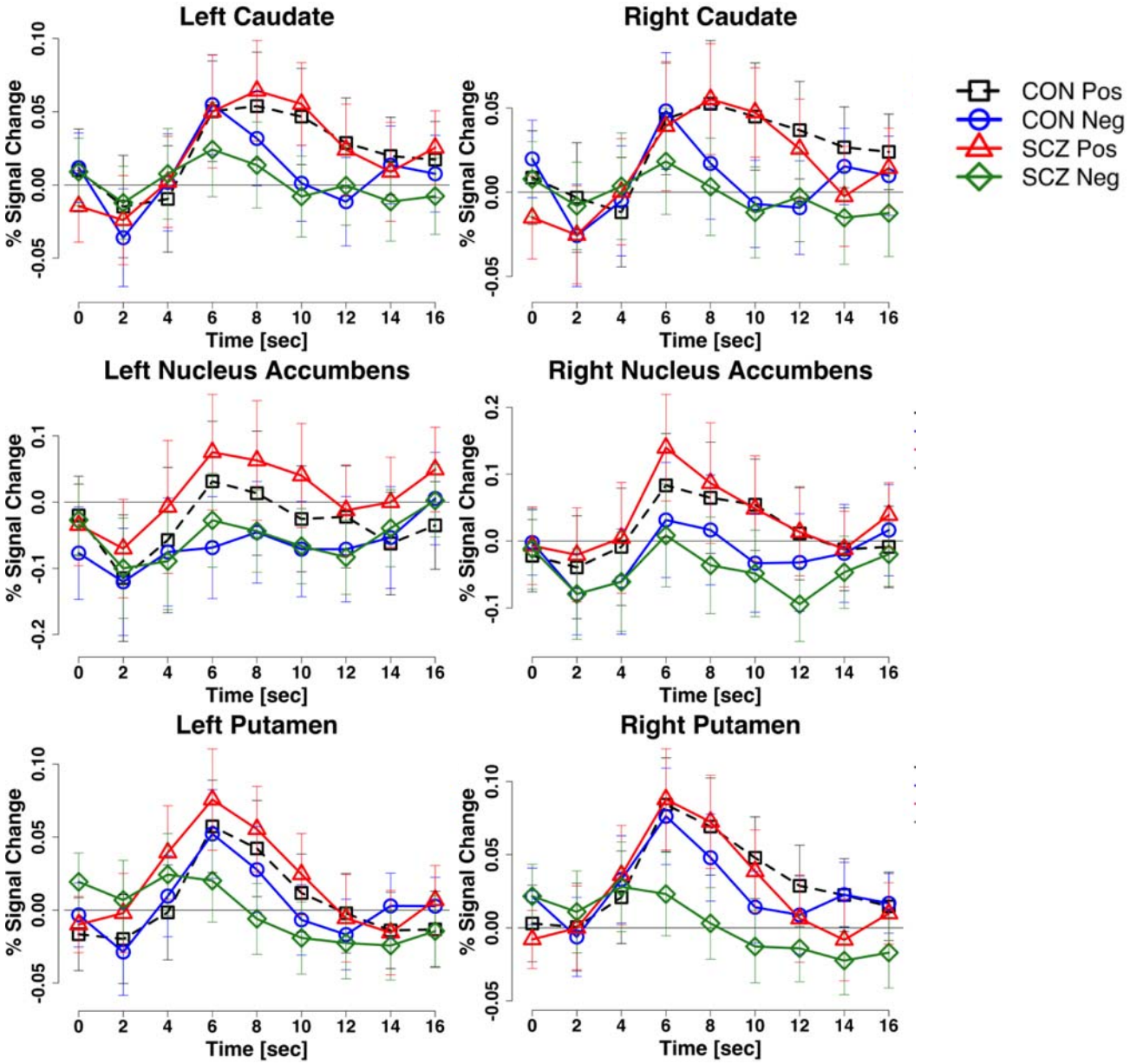

Figure S1. Feedback ANOVA ROI results showing Feedback x Time interactions in all regions.

The whole-brain analysis also identified a number of regions that displayed a significant feedback by time interaction, as shown in Figure S2A. These regions and their activation patterns are summarized in Table S2. Table S2 also includes post-hoc analyses within each stimulus pair, and shows that most of these relationships were driven by the CD and EF pairs more than the AB pair.

Table S2. Feedback ANOVA: Feedback x Time interaction. * $p<.05$, ** $p<.01$, *** $p<.001$, NS: not significant

Table S2A. Regions with greater activation for positive than negative feedback

	Region	BA	Talairach	Voxels	Pattern	Z	AB	CD	EF
L	Amygdala	-	-23, -05, -11	77	Pos > Neg	5.38	NS	*	**
R	Caudate	-	+16, +12, +17	113	Pos > Neg	5.55	*	***	***
L	Caudate	-	-22, -09, +24	33	Pos > Neg	4.07	NS	***	*
R	Cuneus	19	+17, -88, +29	154	Pos > Neg	4.79	NS	*	**
R	Inferior Frontal Gyrus	46	+44, +37, +12	55	Pos > Neg	4.89	NS	NS	**
L	Inferior Parietal Lobule	40	-59, -34, +29	131	Pos > Neg	6.30	*	***	***
R	Inferior Parietal Lobule	40	+55, -27, +34	93	Pos > Neg	4.89	NS	**	**
L	Inferior Parietal Lobule	40	-51, -53, +50	16	Pos > Neg	4.86	NS	NS	*
L	Middle Occipital Gyrus	18	-29, -89, +05	92	Pos > Neg	4.96	NS	**	**
L	Middle Occipital Gyrus	18	-38, -82, -08	28	Pos > Neg	4.81	**	NS	**
L	Middle Temporal Gyrus	39	-45, -72, +20	46	Pos > Neg	4.56	NS	**	*
L	Middle Temporal Gyrus	21	-55, -15, -05	42	Pos > Neg	4.81	*	**	***
R	Middle Temporal Gyrus	21	+56, -08, -04	25	Pos > Neg	4.85	NS	NS	***
L	Middle Temporal Gyrus	37	-52, -53, +01	13	Pos > Neg	3.99	NS	**	**
L	Parahippocampal Gyrus	35	-21, -24, -11	99	Pos > Neg	5.86	NS	***	**
R	Parahippocampal Gyrus	30	+15, -32, -03	34	Pos > Neg	5.64	NS	***	***
L	Postcentral Gyrus	3	-59, -17, +33	55	Pos > Neg	4.98	*	**	***
L	Posterior Cingulate	29	-04, -41, +07	172	Pos > Neg	6.55	NS	***	***
R	Posterior Cingulate	30	+07, -52, +18	147	Pos > Neg	4.97	NS	***	***
R	Precentral Gyrus	6	+57, -10, +36	87	Pos > Neg	5.46	NS	**	**
R	Putamen	-	+28, -16, -08	129	Pos > Neg	5.72	NS	**	**
L	Superior Temporal Gyrus	41	-58, -26, +08	59	Pos > Neg	5.19	NS	NS	**
R	Superior Temporal Gyrus	42	+57, -36, +14	105	Pos > Neg	5.04	NS	NS	***
L	Superior Temporal Gyrus	41	-42, -37, +13	40	Pos > Neg	4.57	NS	**	**
R	Transverse Temporal Gyrus	41	+53, -17, +08	64	Pos > Neg	4.58	NS	NS	**
R	Ventral Striatum	-	+20, +04, -01	200	Pos > Neg	8.39	**	***	***
L	Ventral Striatum	-	-17, +07, +00	183	Pos > Neg	6.33	NS	***	***

Table S2B. Regions with greater activation for negative than positive feedback

	Region	BA	Talairach	Voxels	Pattern	Z	AB	CD	EF
	ACC/preSMA	32	+01, +14, +45	359	Neg > Pos	5.15	NS	**	***
L	Cuneus	18	-11, -85, +12	226	Neg > Pos	5.12	NS	**	***
L	Inferior Frontal Gyrus	47	-46, +14, -04	20	Neg > Pos	4.72	NS	*	NS
L	Inferior Parietal Lobule	40	-38, -39, +41	32	Neg > Pos	4.23	NS	**	*
L	Anterior Insula	13	-34, +18, +07	97	Neg > Pos	4.86	NS	*	**
R	Anterior Insula	13	+32, +17, +11	49	Neg > Pos	4.18	NS	*	*
L	Lingual Gyrus	18	-12, -73, -05	108	Neg > Pos	4.84	NS	**	***
R	Lingual Gyrus	17	+06, -84, +03	126	Neg > Pos	4.46	NS	**	**
R	Superior Frontal Gyrus	6	+07, +07, +60	212	Neg > Pos	5.93	NS	***	***
L	Superior Parietal Lobule	7	-30, -52, +40	36	Neg > Pos	4.13	NS	NS	**
R	Superior Parietal Lobule	7	+28, -57, +44	65	Neg > Pos	4.11	NS	NS	***

Table S2C. Regions with greater activation for negative than positive feedback at peak, but sustained positive responses

	Region	BA	Talairach	Voxels	Pattern	Z	AB	CD	EF
L	Cingulate Gyrus	24	-07, -10, +41	93	Pos Sustained	4.19	NS	**	**
L	Cuneus	19	-14, -81, +30	277	Pos Sustained	5.05	NS	***	***
L	Cuneus	18	-03, -74, +21	208	Pos Sustained	4.91	NS	***	**
L	Fusiform Gyrus	37	-24, -64, -13	23	Pos Sustained	4.33	NS	**	NS
R	Insula	13	+46, +12, -03	44	Pos Sustained	4.75	NS	**	**
L	Insula/Central Operculum	13	-42, -15, +20	39	Pos Sustained	4.65	NS	*	*
R	Lingual Gyrus	18	+25, -74, -10	77	Pos Sustained	4.34	*	*	**
L	Lingual Gyrus	18	-25, -59, +07	62	Pos Sustained	4.82	NS	***	**
L	Medial Frontal Gyrus	6	-05, -18, +62	36	Pos Sustained	4.66	NS	*	***
L	Middle Frontal Gyrus	9	-44, +20, +33	59	Pos Sustained	4.12	NS	*	**
R	Middle Occipital Gyrus	19	+36, -67, +13	57	Pos Sustained	4.31	NS	*	***
R	Middle Temporal Gyrus	37	+50, -62, +10	29	Pos Sustained	4.24	NS	NS	**
L	Postcentral Gyrus	3	-40, -21, +36	152	Pos Sustained	5.37	NS	***	*
L	Posterior Cingulate	30	-09, -61, +14	249	Pos Sustained	5.92	NS	***	***
R	Precentral Gyrus	4	+44, -13, +47	222	Pos Sustained	5.66	NS	**	**
R	Precentral Gyrus	6	+58, -01, +11	70	Pos Sustained	5.88	NS	***	**
L	Precentral Gyrus	4	-46, -08, +47	209	Pos Sustained	5.48	NS	***	***
L	Precentral Gyrus	6	-31, -01, +33	97	Pos Sustained	4.57	NS	*	***
R	Sub-Gyral	40	+27, -40, +54	131	Pos Sustained	4.83	NS	NS	***
L	Superior Frontal Gyrus	6	-13, -03, +63	164	Pos Sustained	5.46	*	**	***
R	Superior Occipital Gyrus	19	+31, -78, +24	95	Pos Sustained	4.40	NS	NS	***
L	Superior Parietal Lobule	7	-22, -48, +60	155	Pos Sustained	5.45	NS	NS	***
R	Supramarginal Gyrus	40	+44, -38, +29	98	Pos Sustained	5.53	NS	*	***
R	Thalamus	-	+02, -26, +12	99	Pos Sustained	5.09	*	***	***

Table S2D. Regions with greater deactivation for negative than positive feedback

	Region	BA	Talairach	Voxels	Pattern	Z	AB	CD	EF
	rACC	32	-01, +42, +05	256	(-) Neg > Pos	6.47	**	***	***
	rACC	24	-02, +28, -03	98	(-) Neg > Pos	5.58	**	**	**
L	Cingulate Gyrus	31	-11, -27, +45	30	(-) Neg > Pos	4.15	NS	**	*
L	Angular Gyrus	19	-39, -72, +34	23	(-) Neg > Pos	4.07	NS	**	NS

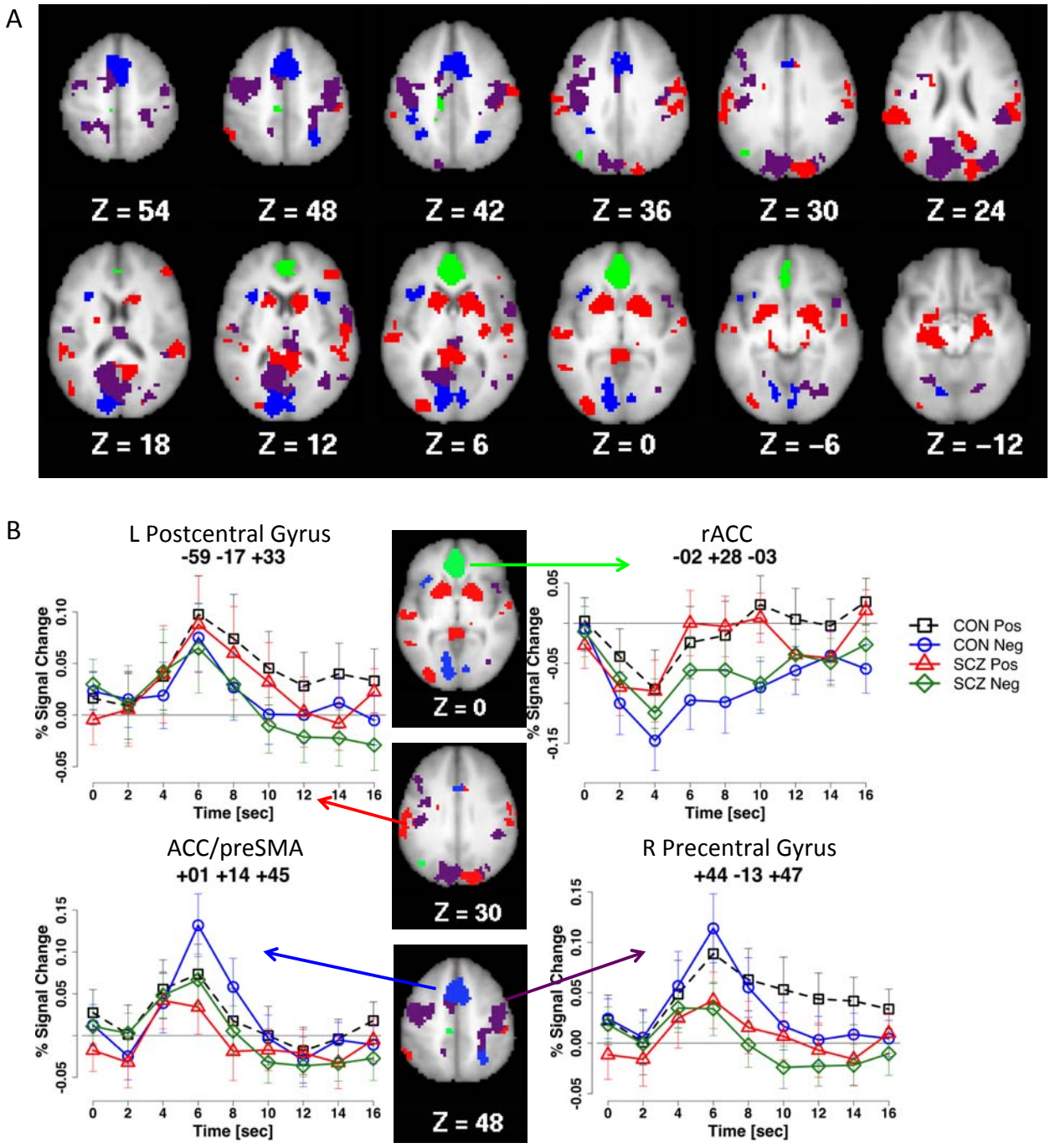

Figure S2. Feedback ANOVA: Feedback x Time interactions. (**A**) Regions with significant Feedback x Time interactions. Red = Positive > Negative; Blue = Negative > Positive; Green = Deactivation, Neg > Pos; Purple = Negative > Positive at peak, with sustained positive response. (**B**) Example timecourses for each response pattern.

Table S3 describes effects and interactions found in the feedback ANOVA analysis that interacted with group. A Time x Group interaction with greater activity in controls than patients

irrespective of feedback type was seen in regions including right inferior parietal lobule and left middle frontal gyrus, while greater activity for patients than controls was seen in occipital regions. Figure S3A shows the few regions that displayed a Feedback x Time x Group interaction. These include regions in left superior and inferior frontal gyri and right precentral gyrus that activated more strongly for negative than positive feedback in controls, with less differentiation between conditions in patients. There were also a few regions displaying a significant Choice x Time x Group interaction, whose activation patterns differed between groups for high- versus low-probability choices regardless of feedback. These regions included right superior frontal gyrus, which activated for BDF choices in controls and ACE choices in patients; cerebellar crus I which showed the opposite patterns, and right angular gyrus and inferior frontal gyrus, which activated for A/C/E choices in patients, but not in controls. Finally, there was a Choice x Feedback x Time x Group interaction in a small set of regions including left insula and VMPFC. Activation timecourses for the VMPFC region are shown in Figure S3B, and reveal deactivation that was strongest for low-probability choices given negative feedback among controls, with little differentiation among conditions in patients.

Table S3. Feedback ANOVA: Interactions with Group

Effect		Region	BA	Talairach	Voxels	Z	Activation Pattern	
							CON	SCZ
Time x Group	R	Lingual Gyrus	19	+18_-61_-6	40	4.31	CON > SCZ	
	L	Cuneus	19	-16_-87_+26	106	5.12	CON > SCZ	
	R	Inferior Parietal Lobule	40	+62_-38_+24	18	4.77	CON > SCZ	
	L	Lingual Gyrus	19	-15_-59_-1	69	4.62	CON > SCZ	
	L	Middle Frontal Gyrus	10	-27_+51_+21	93	5.27	CON > SCZ	
	L	Middle Temporal Gyrus	22	-62_-41_+5	25	4.64	CON > SCZ	
	L	Fusiform Gyrus	19	-25_-89_-18	32	5.15	SCZ > CON	
	R	Fusiform Gyrus	19	+25_-79_-17	19	4.65	SCZ > CON	
	R	Fusiform Gyrus	37	+37_-46_-15	26	4.40	SCZ > CON	
	L	Middle Occipital Gyrus	37	-43_-71_+1	16	4.36	SCZ > CON	
	L	Parahippocampal Gyrus	28	-18_-16_-17	24	4.58	SCZ > CON	
	R	Cuneus	19	+18_-88_+24	144	5.40	SCZ > CON at peak; CON sustained	
	R	Insula	21	+45_-3_-8	21	4.67	SCZ > CON at peak; CON sustained	
	L	Superior Temporal Gyrus	22	-46_-22_+0	25	4.24	SCZ > CON at peak; CON sustained	
	R	Angular Gyrus	39	+57_-63_+34	14	4.39	(-) SCZ > CON	
FB x Time x Group	L	Inferior Frontal Gyrus	13	-27_+14_-12	37	5.04	Neg > Pos	Pos > Neg
	L	Superior Frontal Gyrus	8	-3_+16_+52	42	4.07	Neg > Pos	Neg > Pos
	L	Supramarginal Gyrus	40	-58_-54_+36	17	4.49	Neg > Pos	NS
	R	Precentral Gyrus	4	+37_-19_+51	16	3.83	Neg > Pos at peak; Pos sustained	NS
Choice x Time x Group	L	Genu of Corpus Callosum	-	-15_+25_-3	19	4.46	(-) BDF > ACE	(-) ACE > BDF
	R	Medial Temporal White Matter	-	+38_-33_-5	134	6.08	ACE > BDF	BDF > ACE
	R	Cerebellar Crus I	-	+52_-53_-28	30	5.66	ACE > BDF	BDF > ACE
	R	Superior Frontal Gyrus	10	+29_+60_+4	43	4.93	BDF > ACE	ACE > BDF
	R	Angular Gyrus	40	+56_-57_+36	32	5.28	NS	(+) ACE, (-) BDF
	R	Inferior Frontal Gyrus	46	+52_+37_+11	17	5.37	NS	(+) ACE, (-) BDF
Choice X FB x Time x Group	L	Insula	13	-40_+3_-13	24	4.21	BDF-Neg > ACE > BDF-Pos	BDF-Neg > BDF-Pos > ACE
	L	Lingual Gyrus	18	-19_-66_-10	17	3.69	NS	BDF-Neg > ACE > BDF-Pos
	L	Superior Temporal Gyrus	22	-50_-20_-6	22	4.21	NS	BDF-Pos > BDF-Neg > ACE
	L	Ventromedial PFC	10	-8_+40_-6	16	4.56	(-) BDF-Neg > BDF-Pos > ACE	NS

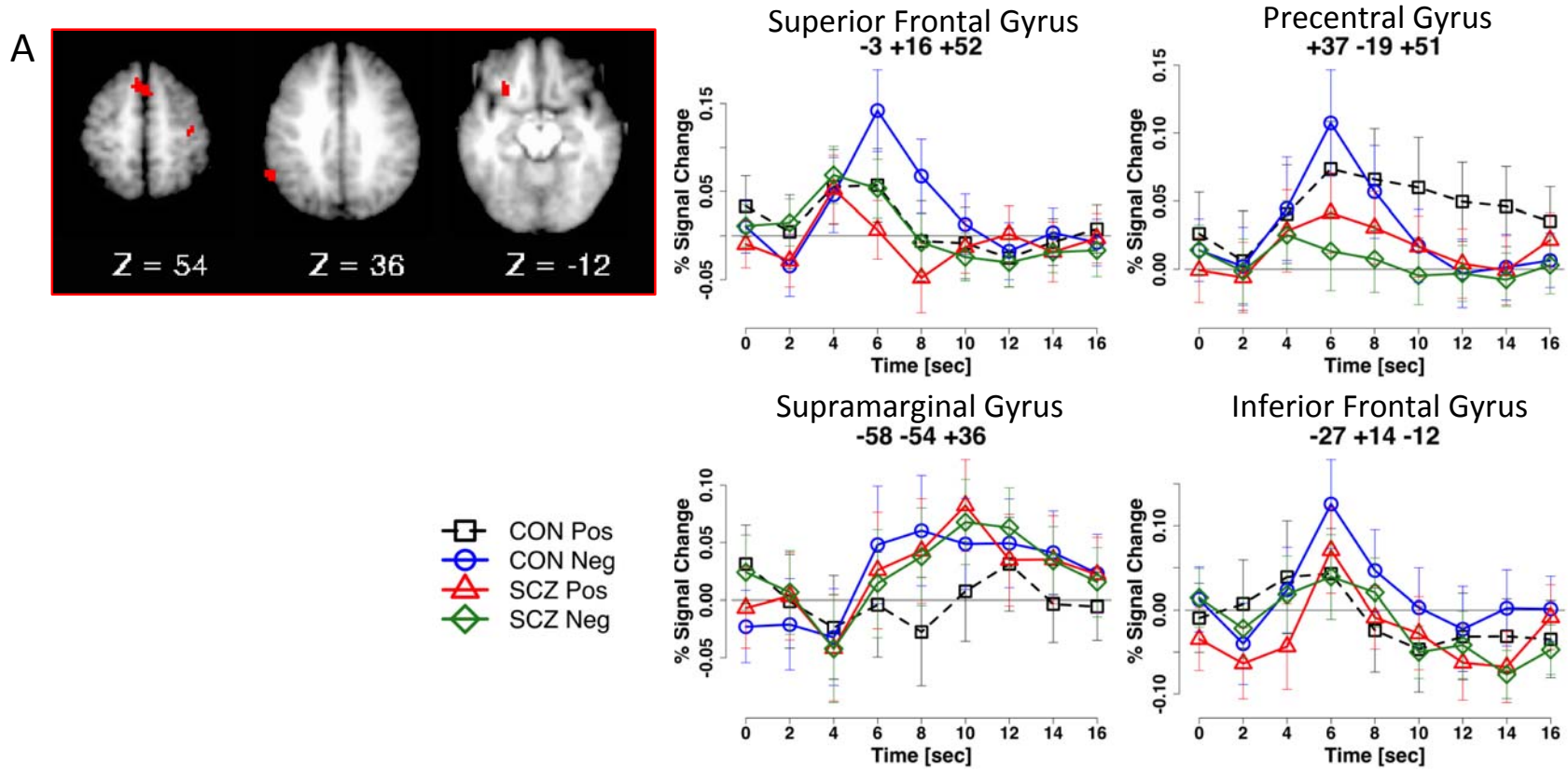

Figure S3. Feedback ANOVA: Interactions with Group. (**A**) Regions with Feedback x Time x Group interactions.

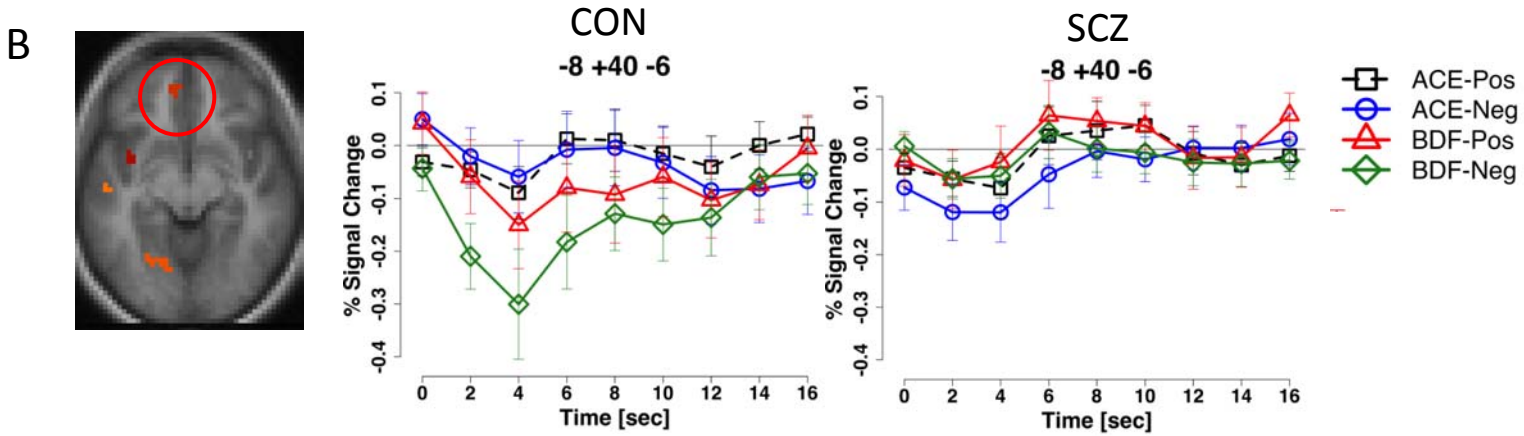

Figure S3. Feedback ANOVA: Interactions with Group. (**B**) VMPFC region with a Choice x Feedback x Time x Group interaction.

Overall, the feedback ANOVA revealed robust main effects of feedback that did not differ between groups in most regions associated with reward or cognitive control. Striatal regions activated more strongly for positive than negative feedback, while cognitive control regions showed the opposite pattern. This pattern is highly similar to that seen in the prediction error analysis. In terms of group effects, a few cortical regions demonstrated reduced feedback responses among patients overall, while a set of posterior regions activated more strongly in patients overall. A small region in VMPFC showed responses that varied with both choice and feedback among controls, but were absent in patients. Overall, there were few group differences that were robust and showed an interpretable pattern with respect to choice and feedback type, and no evidence was found for altered striatal responses to feedback among patients.

Choice Analyses

ANOVA analysis of choice-related activity with all trials

This analysis examined activity associated with choices of high vs. low-probability stimuli, using a repeated-measures ANOVA with Choice (A/C/E, B/D/F) and Time (1-9) as within-subjects factors and Group (CON, SCZ) as a between-subjects factor. Stimulus pairs were combined for the purposes of this analysis because a number of subjects had too few “B” choices to model activity for each pair type separately; effects of stimulus pair were evaluated in a separate analysis reported in the main text.

A priori ROI analysis within bilateral caudate, putamen, and nucleus accumbens revealed significant main effects of time in all regions, but no significant interactions with time. Whole-brain analysis revealed a number of regions demonstrating a significant Choice x Time interaction, shown in Figure S4A and Table S4. This analysis revealed a significant choice x time effect in several members of the cognitive control network including bilateral DLPFC, posterior parietal cortex, cerebellum, and ACC/preSMA. All of these regions demonstrated greater activation for low-reward than high-reward choices for both patients and controls (Figure

S4B). In addition, a region in dorsomedial prefrontal cortex demonstrated greater deactivation for high-probability than low-probability choices in both groups. Table S4 also includes post-hoc tests conducted within each stimulus pair, and shows that most of these patterns were driven by the AB and/or EF pairs, with little contribution of the CD pair.

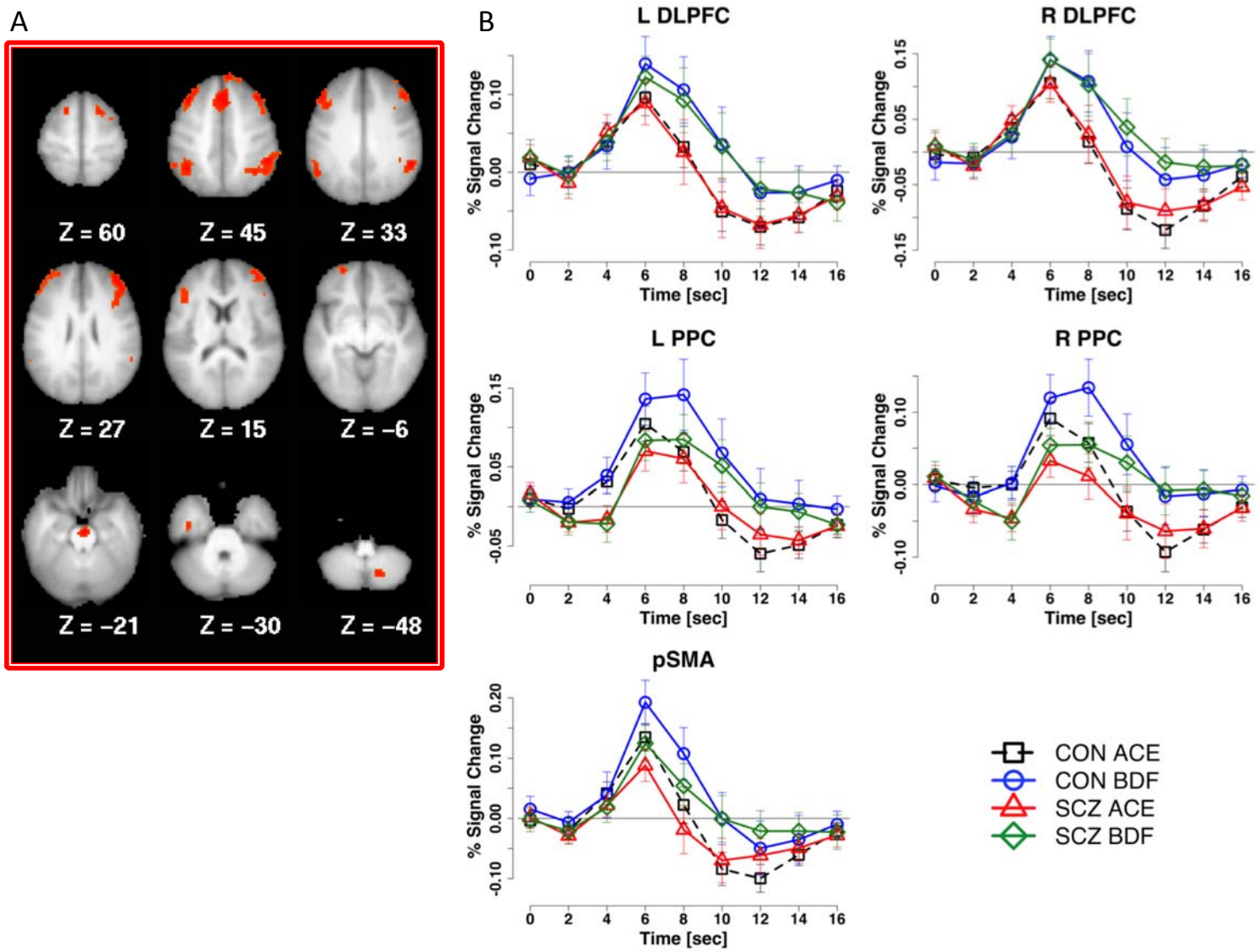

Figure S4. Choice ANOVA results: main effect of choice in the full acquisition phase. (**A**) Regions demonstrating a main effect of choice on whole-brain analysis ($Z \geq 3$, $n \geq 13$). All regions showed greater activity for incorrect than correct choices. (**B**) Example timecourses for cognitive control regions, demonstrating greater activation for incorrect than correct choices in both patients and controls.

Time x Group interactions (Table S4) were seen in regions in bilateral superior parietal lobule, left superior frontal gyrus, and cuneus, which demonstrated greater activation overall (i.e. for both choice types) among controls than patients. Greater activation for patients than controls was seen in bilateral cuneus, left inferior parietal lobule, and right superior parietal lobule.

Table S4. Choice ANOVA: Regions demonstrating main effects

Effect		Region	BA	Coordinates	# Voxels	Z	Pattern	AB	CD	EF
Choice x Time	R	Cerebellar Tonsil	-	+16, -66, -49	19	4.32	BDF>ACE	NS	NS	***
	L	Middle Frontal Gyrus	9	-40, +27, +33	267	5.12	BDF>ACE	NS	NS	***
	R	Middle Frontal Gyrus	9	+39, +28, +34	366	6.61	BDF>ACE	***	NS	***
	R	Pons	-	+2, -19, -20	23	5.09	BDF>ACE	NS	NS	***
	L	Middle Frontal Gyrus	10	-26, +54, -7	15	4.62	BDF>ACE	NS	NS	***
	R	Inferior Parietal Lobule	40	+41, -53, +44	285	6.21	BDF>ACE	***	NS	***
	L	Inferior Parietal Lobule	40	-45, -51, +41	236	5.00	BDF>ACE	***	NS	***
		Medial Frontal Gyrus	8	+0, +21, +46	228	4.71	BDF>ACE	***	NS	**
	L	Middle Frontal Gyrus	6	-19, +11, +62	18	4.96	BDF>ACE	NS	NS	***
	R	Superior Frontal Gyrus	6	+18, +11, +63	44	5.84	BDF>ACE	*	NS	***
	R	Medial Frontal Gyrus	8	+6, +49, +42	33	4.43	(-) ACE>BDF	NS	NS	***
	L	Uncus	20	-38, -15, -28	23	4.31	ACE: early peak, then (-)	NS	NS	***
Time x Group	R	Precuneus	7	+27, -66, +30	16	3.87	CON > SCZ	***	***	**
	L	Superior Frontal Gyrus	10	-18, +52, -3	42	4.95	CON > SCZ	***	**	***
	L	Superior Frontal Gyrus	6	-1, +19, +58	94	3.37	CON > SCZ	*	NS	***
	R	Superior Parietal Lobule	7	+15, -67, +59	63	4.43	CON > SCZ	***	***	***
	R	Cuneus	19	+14, -91, +24	43	4.14	SCZ > CON	***	***	**
	L	Cuneus	19	-21, -91, +26	34	4.71	SCZ > CON	***	***	***
	L	Inferior Parietal Lobule	40	-52, -32, +54	14	3.65	SCZ > CON	***	***	**
	R	Superior Parietal Lobule	7	+32, -45, +61	15	3.13	SCZ > CON	***	***	*
	L	Insula	13	-44, -19, +0	13	3.50	(-) CON > SCZ	NS	***	**
	R	Inferior Temporal Gyrus	20	+55, -23, -18	18	3.38	(+) SCZ, (-)CON	***	NS	*

Regions showing a significant Choice x Time x Group interaction are shown in Figure S5 and Table S5. The majority of these regions, those predominantly located in the cerebellum and occipital lobe, activated more strongly for low- than high-probability

choices in controls, but for high- than low-probability choices in patients. Another subset of regions including bilateral precuneus also showed greater activation for low-probability choices in controls, but no differentiation between choice types in patients. Finally, regions including right superior frontal gyrus showed greater activation for high- than low-probability choices in patients, and no differentiation among controls. Similar patterns were seen in the analysis focusing on the AB pair below. Notably, no group differences were seen in striatal regions.

Table S5. Choice ANOVA: regions demonstrating Choice x Time x Group interactions

	Region	BA	Talairach	Voxels	Z	Post-hoc	
						CON	SCZ
L	Cerebellar VI	-	-31_-46_-26	112	6.10	BDF > ACE	ACE > BDF
L	Fusiform Gyrus	-	-24_-62_-13	42	4.00	BDF > ACE	ACE > BDF
R	Cerebellar Vermis VI	-	+3_-65_-24	134	4.28	BDF > ACE	ACE > BDF
L	Crus I	-	-29_-72_-33	34	3.88	BDF > ACE	ACE > BDF
R	Cerebellar VI	-	+40_-43_-34	57	5.11	BDF > ACE	ACE > BDF
R	Cerebellar IX	-	+10_-51_-39	96	5.09	BDF > ACE	ACE > BDF
R	Fusiform Gyrus	19	+27_-74_-12	270	6.92	BDF > ACE	ACE > BDF
R	Inferior Parietal Lobule	40	+52_-31_+54	17	4.52	BDF > ACE	ACE > BDF
L	Middle Occipital Gyrus	18	+24_-90_+6	98	4.00	BDF > ACE	ACE > BDF
L	Precentral Gyrus	4	-33_-27_+67	34	3.87	BDF > ACE	ACE > BDF
L	Rectal Gyrus	11	-3_+23_-22	16	4.16	BDF > ACE	ACE > BDF
R	Superior Frontal Gyrus	9	+19_+51_+31	16	3.59	BDF > ACE	ACE > BDF
R	MTL/Occipital WM	-	+32_-35_+6	462	6.63	BDF > ACE	ACE > BDF
L	MTL/Occipital WM	-	-26_-45_+11	801	6.17	BDF > ACE	ACE > BDF
L	Superior Parietal Lobule	7	-25_-59_+56	30	4.30	BDF > ACE	ACE > BDF
R	Thalamus	-	+1_-26_+15	37	4.39	BDF > ACE	ACE > BDF
L	Cerebellar Crus I	-	-26_-75_-22	13	2.99	BDF > ACE	NS
R	Cerebellar Vermis VI	-	-1_-85_-22	31	4.25	BDF > ACE	NS
R	Cingulate Gyrus	23	-2_-21_+28	24	4.48	BDF > ACE	NS
R	Cuneus	23	+10_-75_+10	17	2.91	BDF > ACE	NS
R	Precuneus	7	+28_-43_+44	15	3.74	BDF > ACE	NS
L	Precuneus	7	+12_-69_+49	49	3.95	BDF > ACE	NS
L	Superior Frontal Gyrus	10	+29_+45_+18	55	4.19	BDF > ACE	NS
L	Superior Frontal Gyrus	9	-27_+45_+32	14	3.86	BDF > ACE	NS
R	Superior Parietal Lobule	7	+27_-61_+53	14	3.90	BDF > ACE	NS
L	Cerebellar Peduncle	-	-19_-56_-40	42	4.94	ACE > BDF early	ACE > BDF
R	Cingulate WM	-	+19_+0_+32	41	3.85	ACE > BDF early	ACE > BDF
R	Cerebellar Culmen	-	+8_-37_-13	16	3.42	NS	ACE > BDF
R	Superior Frontal Gyrus	10	+29_+59_+2	24	4.35	NS	ACE > BDF
L	Frontal WM	-	-18_+25_+16	19	3.62	NS	ACE > BDF
R	Angular Gyrus	39	+57_-59_+34	14	4.86	NS	(-) ACE > BDF

R = Right, L = Left, WM = White Matter, BA = Brodmann Area, MTL = Medial Temporal Lobe

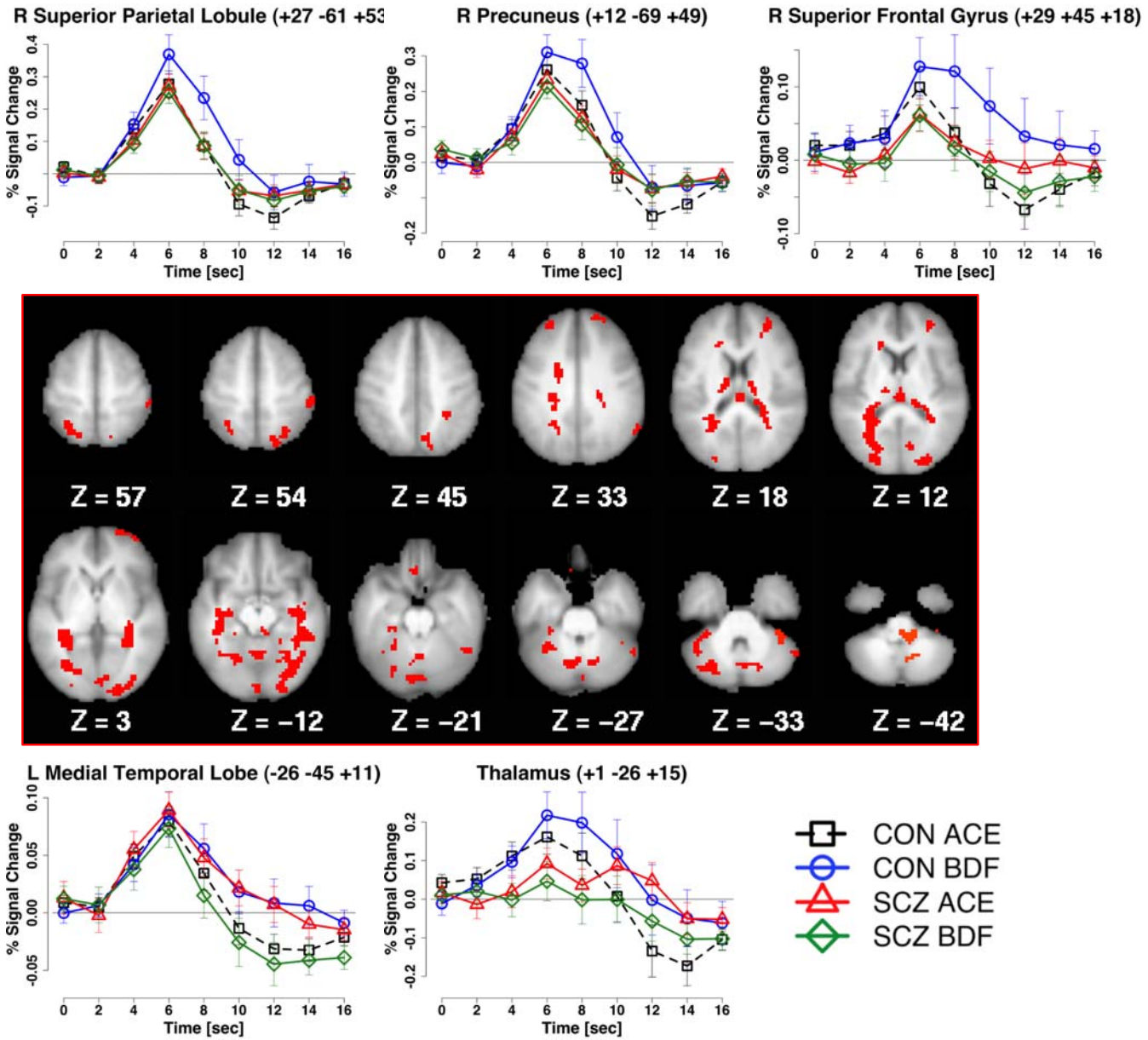

Figure S5. Choice ANOVA: Regions with Choice x Time x Group interactions

ANOVA analysis of choice-related activity focusing on AB pair

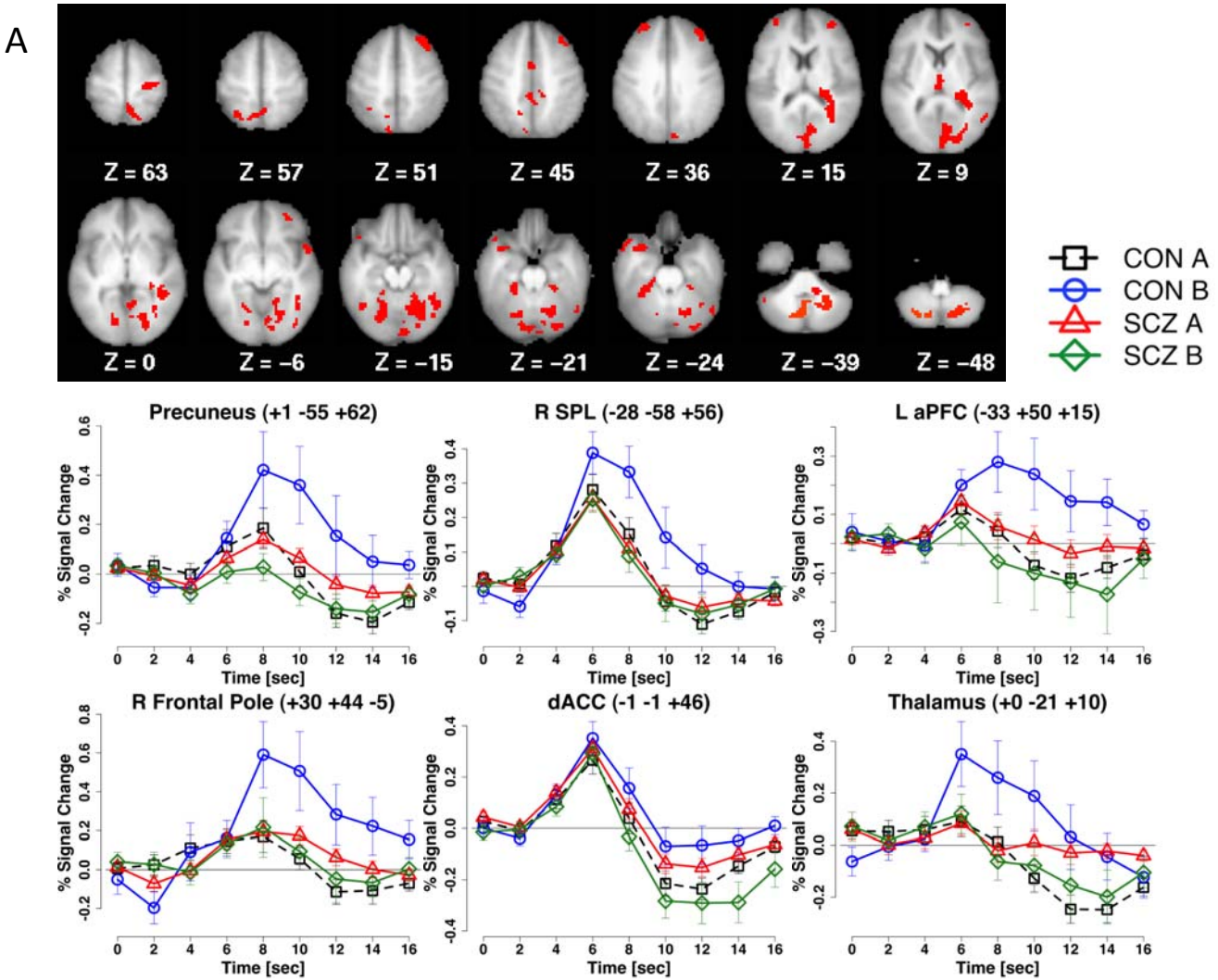

Figure S6. Choice ANOVA: within AB pair. (**A**) Regions and example timecourses for significant Choice x Time x Group interactions.

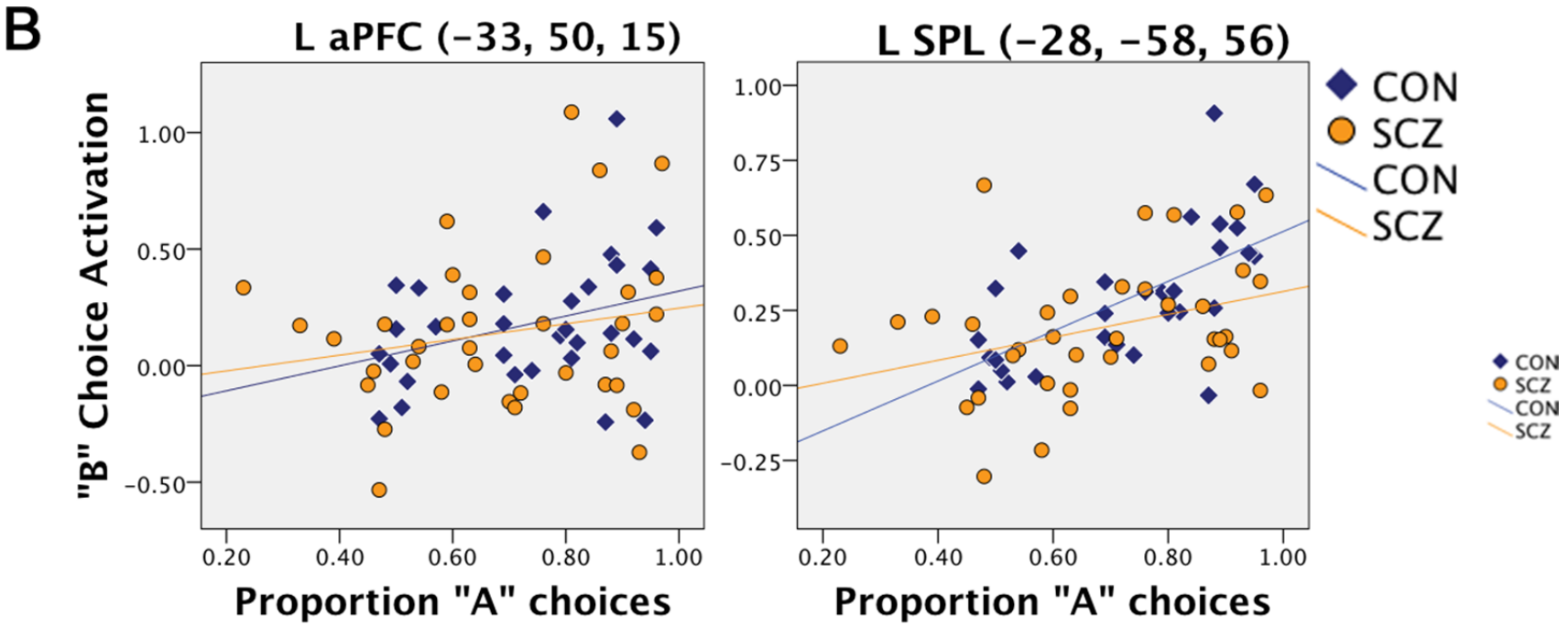

Figure S6. Choice ANOVA: within AB pair. (**B**) Correlations between activation for B choices and performance on the AB pair (proportion of "A" choices during the full acquisition phase), or early Win-Stay performance (proportion of wins followed by stays during the first 2 blocks).

Choice-related activity as a function of learning

Table S6. Choice-related activity within the early learning phase

Effect		Region	BA	Talairach	Voxels	Z	Pattern		Post-Hoc	
							CON	SCZ	CON	SCZ
Choice x Time	R	Cuneus	18	+11_-70_+13	523	5.02	ACE > BDF		*	*
	L	Inferior Frontal Gyrus	47	-29_+28_-8	14	4.28	ACE > BDF		*	*
	L	Inferior Frontal Gyrus	10	-36_+43_+0	41	4.90	ACE > BDF		*	*
	R	Insula	13	+39_-3_+7	104	4.63	ACE > BDF		*	*
	R	Middle Occipital Gyrus	19	+40_-66_+13	15	4.04	ACE > BDF		*	*
	R	Postcentral Gyrus	3	+57_-13_+21	137	6.37	ACE > BDF		*	*
	L	Posterior Cingulate	30	-17_-62_+7	299	5.23	ACE > BDF		*	*
	L	Caudate	-	-12_+22_+06	155	5.27	ACE > BDF		NS	*
	R	Caudate	-	+16_+27_+03	99	4.64	ACE > BDF		NS	*
	L	Cerebellar Peduncle	-	-26_-51_-42	20	4.70	ACE > BDF		NS	*
	R	Fusiform Gyrus	37	+37_-60_-13	47	4.83	ACE > BDF		NS	*
	L	Middle Occipital Gyrus	19	-35_-88_+11	14	4.11	ACE > BDF		NS	*
	R	Middle Frontal Gyrus	9	+35_+26_+28	14	3.63	ACE > BDF		NS	*
	L	Middle Frontal Gyrus	46	-40_+30_+19	44	4.56	BDF > ACE		*	*
	L	Precentral Gyrus	6	-52_+4_+34	18	4.31	BDF > ACE		*	*
	L	Angular Gyrus	39	-43_-76_+32	25	4.52	(-) BDF > ACE		*	*
	R	Posterior Insula	13	+42_-28_+15	44	4.63	(-) BDF > ACE		*	*
	L	Middle Temporal Gyrus	39	-51_-73_+13	30	4.82	(-) BDF > ACE		*	*
	R	Superior Temporal Gyrus	21	+53_-3_-9	17	4.65	(-) BDF > ACE		*	*
	R	Superior Temporal Gyrus	22	+70_-36_+7	26	5.93	(-) BDF > ACE		*	*
	L	Superior Temporal Gyrus	22	-54_-37_+10	184	5.99	(-) BDF > ACE		*	*
Time x Group	L	Thalamus	-	-1_-31_+11	43	3.36	CON > SCZ		-	-
	L	Precuneus	7	-25_-67_+36	62	4.82	CON > SCZ		-	-
	L	Superior Parietal Lobule	7	-29_-59_+60	27	3.45	CON > SCZ		-	-
	L	Inferior Parietal Lobule	40	-47_-43_+42	43	4.30	CON > SCZ		-	-
	R	Superior Frontal Gyrus	6	+0_+19_+57	169	5.01	CON > SCZ		-	-
	R	Superior Parietal Lobule	7	+25_-62_+48	345	5.67	CON > SCZ		-	-
	R	Precuneus	7	+27_-68_+37	16	3.88	CON > SCZ		-	-
	R	Cerebellar VIIIa	-	+32_-43_-51	15	3.66	CON > SCZ		-	-
	R	Middle Frontal Gyrus	9	+38_+22_+27	21	3.90	CON > SCZ		-	-
	R	Inferior Frontal Gyrus	45	+53_+16_+4	28	4.92	CON > SCZ		-	-
Choice x Time x Group	R	Cerebellar Crus I	-	+55_-61_-30	14	5.54	BDF > ACE	ACE > BDF	*	*
	R	Midbrain	-	+1_-32_-11	14	3.78	BDF > ACE	ACE > BDF	*	*
	R	Thalamus	-	+16_-19_+19	29	4.27	-	ACE > BDF	NS	*
	R	Precentral Gyrus	4	+55_-14_+42	22	4.18	ACE > BDF	-	*	NS

Medication Effects: We converted antipsychotic doses to standard chlorpromazine dose-equivalents (18), and conducted correlations between these doses and our behavioral and neuroimaging measures of interest. Behaviorally, there was a significant relationship between medication dose and AvoidD (rho = .408, $p<.02$), wherein AvoidD scores were higher for larger medication doses. Dose did not correlate with ChooseC, gain or loss learning rate, or anhedonia/avolition. In the neuroimaging data, we examined all regions with significant group differences in the analyses above to determine whether the effect that differed between groups correlated with medication dose. None of the examined relationships were significant. Next, we conducted the same ROI and whole-brain correlations as described for the anhedonia/avolition analysis above, which also failed to yield significant results.

Table S7. Correlations between individual difference variables and prediction error activity in striatal ROIs

Region	**Avg. AB Training Accuracy**		**Choose C**		**Avoid D**		**Gain Learning Rate**		**Loss Learning Rate**		**Self-reported Anhedonia / Avolition**		**Clinician Rated Anhedonia / Avolition**	
Learners Only	***r***	***p***	***r***	***p***	***r***	***p***	***r***	***p***	***r***	***p***	***r***	***p***	***r***	***p***
Left Caudate	0.08	0.70	0.05	0.82	0.02	0.93	0.19	0.35	0.02	0.94	0.30	0.14	0.45*	0.02
Right Caudate	0.40	0.86	0.07	0.75	0.00	1.00	0.21	0.31	0.04	0.83	0.27	0.18	0.42*	0.03
Left Nucleus Accumbens	-0.01	0.97	0.17	0.42	-0.10	0.65	0.14	0.51	-0.06	0.78	0.06	0.76	0.35*	0.08
Right Nucleus Accumbens	0.06	0.76	0.18	0.38	0.07	0.75	0.38	0.06	0.16	0.42	-0.18	0.37	0.04	0.84
Left Putamen	-0.06	0.59	-0.05	0.80	-0.06	0.76	-0.08	0.69	-0.01	0.97	0.25	0.22	0.44*	0.02
Right Putamen	-0.03	0.81	0.04	0.85	-0.03	0.87	0.01	0.95	0.01	0.96	0.19	0.34	0.40*	0.04
Full Schizophrenia Sample														
Left Caudate	-0.02	0.92	-0.13	0.45	0.08	0.65	0.00	0.98	-0.14	0.20	0.06	0.71	0.36*	0.03
Right Caudate	-0.06	0.44	-0.07	0.68	0.04	0.81	-0.05	0.76	-0.04	0.59	0.03	0.88	0.35*	0.03
Left Nucleus Accumbens	-0.13	0.72	-0.15	0.37	0.02	0.89	0.03	0.84	-0.20	0.12	-0.14	0.40	0.11	0.53
Right Nucleus Accumbens	-0.13	0.30	-0.04	0.81	0.14	0.41	0.07	0.66	0.03	0.43	-0.25	0.13	0.02	0.89
Left Putamen	-0.06	0.71	0.02	0.91	0.06	0.74	-0.20	0.24	-0.15	0.19	0.01	0.96	0.23	0.18
Right Putamen	-0.14	0.41	-0.06	0.73	0.05	0.78	-0.20	0.24	-0.12	.24	-0.11	0.53	0.19	0.26

* Greater clinical rated anhedonia/amotivation related to greater striatal response (opposite of prediction), but did not pass FDR correction.

Table S8. Regions showing correlations between positive feedback related activity with self-reported anhedonia/avolition

Region	**BA**	**X**	**Y**	**Z**
Left Inferior Occipital Gyrus	37	-40	-63	-6
Left Caudate		-6	4	3
Left Middle Occipital Gyrus	19	52	-64	3
Left Middle Temporal Gyrus	22	-56	-47	5
Right Middle Frontal Gyrus	9	43	8	29
Left Middle Occipital Gyrus	18	-23	84	20
Right Precuneus	31	23	-75	26
Left Middle Frontal Gyrus	6	-45	-1	29
Right Precentral Gyrus	4	39	-11	53
Left Precentral Gyrus	6	-46	-6	54
Left Inferior Parietal Lobule	40	-42	-36	58
Left Superior Frontal Gyrus	6	-3	14	64
Paracentral Lobule	4	0	-31	70
Left Postcentral Gyrus	3	-18	-37	70

Supplemental References

1. First M, Spitzer R, Gibbon M, Williams J (2001): *Structured clinical interview for DSM-IV-TR axis I disorders-patient edition*. Biometrics Research Department, New York State Psychiatric Institute.
2. Andreasen NC (1983): The scale for the assessment of positive symptoms (SAPS). Iowa City: University of Iowa.
3. Andreasen NC (1983): The scale for the assessment of negative symptoms (SANS). Iowa City: University of Iowa.
4. Kirkpatrick B, Strauss GP, Nguyen L, Fischer BA, Daniel DG, Cienfuegos A, et al. (2011): The brief negative symptom scale: psychometric properties. *Schizophr Bull*. 37:300-305.
5. Chapman LJ, Chapman JP (1978): The revised physical anhedonia scale [Unpublished Test]: University of Wisconsin: Madison.
6. Chapman LJ, Chapman JP, Raulin ML (1976): Scales for physical and social anhedonia. *J Abnorm Psychol*. 85:374-382.
7. Gard DE, Kring AM, Gard MG, Horan WP, Green MF (2007): Anhedonia in schizophrenia: distinctions between anticipatory and consummatory pleasure. *Schizophr Res*. 93:253-260.
8. Snaith RP, Hamilton M, Morley S, Humayan A, Hargreaves D, Trigwell P (1995): A scale for the assessment of hedonic tone the Snaith-Hamilton Pleasure Scale. *Br J Psychiatry*. 167:99-103.
9. Starkstein SE, Mayberg HS, Preziosi TJ, Andrezejewski P, Leiguarda R, Robinson RG (1992): Reliability, validity, and clinical correlates of apathy in Parkinson's disease. *J Neuropsychiatry Clin Neurosci*. 4:134-139.
10. Frank M, Seeberger LC, O'reilly RC (2004): By carrot or by stick: cognitive reinforcement learning in parkinsonism. *Science*. 306:1940-1943.
11. Rossion B, Pourtois G (2004): Revisiting Snodgrass and Vanderwart's object pictorial set: the role of surface detail in basic-level object recognition. *Perception*. 33:217-236.
12. Bandettini PA, Jesmanowiz J, Wong EC, Hyde JS (1993): Processing strategies for time-course data sets in functional MRI of the human brain. *Magnetic Resonance in Medicine*. 30:161-173.
13. Friston KJ, Jezzard P, Turner R (1994): The analysis of functional MRI time series. *Human Brain Mapping*. 2:1-45.
14. Snyder AZ (1996): Difference image versus ratio image error function forms in PET-PET realignment. In: Bailer D, Jones T, editors. *Quantification of Brain Function Using PET*. San Diego: Academic Press.
15. Woods RP, Cherry SR, Mazziotta JC (1992): Rapid automated algorithm for aligning and reslicing PET images. *Journal of Computer Assisted Tomography*. 16:620-633.
16. Frank MJ, Moustafa AA, Haughey HM, Curran T, Hutchison KE (2007): Genetic triple dissociation reveals multiple roles for dopamine in reinforcement learning. *Proc Natl Acad Sci U S A*. 104:16311-16316.
17. Schwarz G (1978): Estimating the dimension of a model. *Annals of Statistics*. 6:461-464.
18. Gardner DM, Murphy AL, O'Donnell H, Centorrino F, Baldessarini RJ (2010): International consensus study of antipsychotic dosing. *Am J Psychiatry*. 167:686-693.